Communication

Synthesis of (–)-Mitrephorone A via a Bio-inspired Late Stage C–H Oxidation of (–)-Mitrephorone B

Lukas Anton Wein, Klaus Wurst, Péter Angyal, Lara Weisheit, and Thomas Magauer

J. Am. Chem. Soc., **Just Accepted Manuscript** • DOI: 10.1021/jacs.9b11646 • Publication Date (Web): 26 Nov 2019

Synthesis of (–)-Mitrephorone A via a Bio-inspired Late Stage C–H Oxidation of (–)-Mitrephorone B

Lukas Anton Wein,[†] Klaus Wurst,[‡] Peter Angyal,[§] Lara Weisheit,[†] and Thomas Magauer*,[†]

[†]Institute of Organic Chemistry and Center for Molecular Biosciences, Leopold-Franzens-University Innsbruck, Innrain 80–82, 6020 Innsbruck, Austria

[‡]Institute of General, Inorganic and Theoretical Chemistry, Leopold-Franzens-University Innsbruck, Innrain 80−82, 6020 Innsbruck, Austria

[§]Institute of Organic Chemistry, Research Centre for Natural Sciences, Magyar tudósok körútja 2, 1117 Budapest, Hungary

Supporting Information Placeholder

ABSTRACT: We present a bio-inspired late stage C–H oxidation of the *ent*-trachylobane natural product mitrephorone B to mitrephorone A. The realization of this unprecedented transformation was accomplished by either an iron-catalyzed or electrochemical oxidation and enabled access to the densely substituted oxetane in one step. Formation of mitrephorone C, which is lacking the central oxetane unit but features a keto-function at C2, was not formed under these conditions.

The *ent*-trachylobane natural products mitrephorone A (**1**), B (**2**) and C (**3**) are structurally related to the diterpenoids *ent*-atiserene, *ent*-beyerene, and *ent*-kaurene, but they display a rare and synthetically challenging oxidation pattern (Scheme 1).[1,2] An initial bioactivity screen revealed moderate anti-microbial and anti-cancer activities for **1**–**3**.[2] The proposed biosynthesis begins with the cyclization of geranylgeranyl pyrophosphate (GGPP, C_{20}) to the *ent*-pimarenyl carbocation **4**. The mechanism for the conversion of **4** into the *ent*-trachylobane skeleton **5** was clarified by Tantillo and excludes the intermediacy of a previously postulated secondary carbocation.[3] After the initial cyclization phase, **5** is enzymatically postmodified. As shown for the formation of mitrephorone B (**2**), it is reasonable that either the *trans*-decalin framework is oxidized first (Path A) or that functionalization of C19 to give *ent*-trachyloban-19-oic acid (**6**) precedes this event (Path B). At the outset of this project, we hypothesized that **2** represents the pivotal intermediate from which **1** and **3** are generated via selective oxidation. Based on this consideration and our continued interest to constructing synthetically challenging oxetanes,[4] we envisioned investigation of this oxidation process in the chemical laboratory. Notably, mimicking the putative oxidation of mitrephorone B (**2**) to mitrephorone A (**1**) would allow us to circumvent the limited substrate scope generally associated with conventional oxetane formation methods such as ring-expansion, [2+2]-cycloaddition, and nucleophilic displacement reactions.[5,6] Carreira recently disclosed the synthesis of **1** employing an elegant Umpolung strategy.[5] Here we present the first total synthesis of mitrephorone B (**2**) and show its conversion to mitrephorone A (**1**) via a bio-inspired late-stage C–H oxidation.[7,8]

Retrosynthetic bond disconnections of our initial target, mitrephorone B (**2**), revealed tricyclo-[3.2.1.0^{2,7}]oct-3-ene **7** as the precursor. For the installation of this motif, **7** was traced back to 5-vinyl-1,3-cyclohexadiene **8** by employing an intramolecular retro-Diels–Alder (IMDA) reaction.

Scheme 1. Schematic Biosynthesis of Mitrephorone A (1), B (2), and C (3) and Retrosynthetic Analysis.

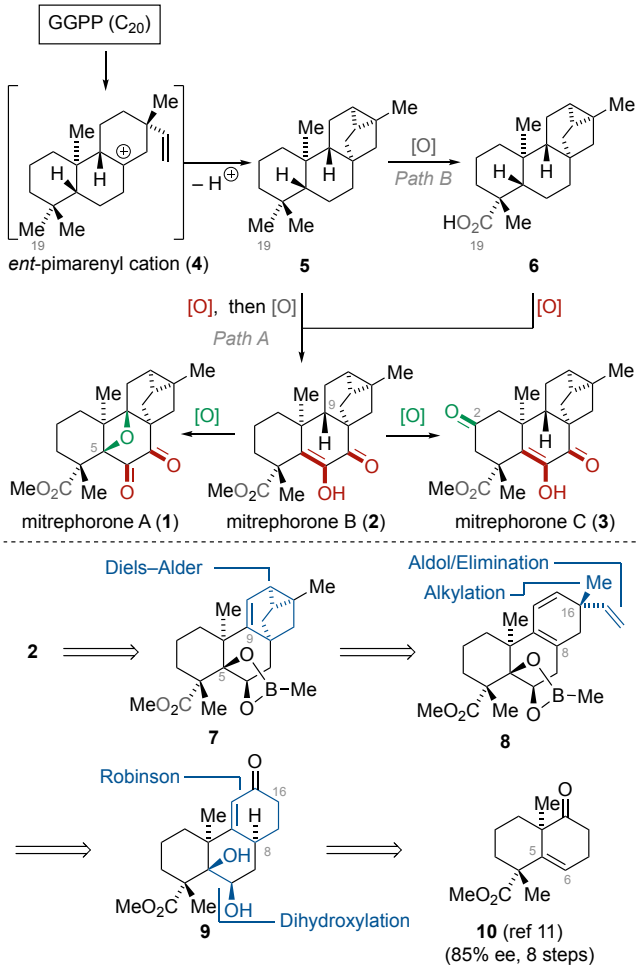

This powerful type of IMDA was previously emulated in related systems by Trauner[9] and has proven its efficiency in the synthesis of **1**.[5] Removal of the C16 quaternary stereocenter revealed enone **9**, which contains the retron for a simplifying Robinson annulation.[10] Further disconnection of **9** generated known ketone **10**[11] as the ideal starting point for our investigations.

As shown in Scheme 2, asymmetric synthesis of **10** was carried out on multigram scale (4.4 g) in good overall yield. The Upjohn dihydroxylation of the neopentylic alkene was exceptionally challenging and no conversion of the starting material took place at ambient temperature. Fortunately, it was found that 1,2-diol **11** was obtained in good yield and as a single diastereomer by conducting the dihydroxylation at elevated temperature (90 °C) using 1,4-diazabicyclo[2.2.2]octane (DABCO) as a crucial additive in this transformation.[12] The early dihydroxylation of the C5–C6 alkene enabled investigation of the limitation of oxetane formation via nucleophilic substitution and revealed valuable information about the structural requirements for the realization of the C–H oxidation (*vide infra*). Conversion of **11** to tricyclic enone **9** was accomplished by employing a two-step Robinson annulation protocol.[10] First, **11** was activated by installation of a β-keto aldehyde (NaH, methyl formate). Subsequent exposure of this intermediate to methyl vinyl ketone (MVK), followed by addition of sodium methoxide gave **9** in reproducibly good yield (57% over two steps) and excellent diastereoselectivity (20:1).[13]

Further functionalization and installation of the quaternary carbon center at C16 required protection of the 1,2-diol motif. From a survey of protecting groups (e.g. dialkylsilylenes, acetonides, benzylidene acetal, cyclic carbonates), installation of a rarely used cyclic boronic ester[14] emerged as the sole solution ($MeB(OH)_2$, benzene, 30 °C). The boronic ester was stable enough to undergo the following alkylation/aldol sequence and was amenable to selective cleavage at a later stage. While the α-methylation (LiHMDS, MeI, 82%) proceeded efficiently, all attempts to realize a subsequent direct α-vinylation[15] resulted in complex reaction mixtures and low isolated yields. Therefore, a two-step protocol was employed. First, aldol reaction with acetaldehyde as an inexpensive C2 synthon (LDA, TMEDA, acetaldehyde, –78 °C)[16] gave **12**, whose single crystal structure validated the depicted stereochemistry. Sequential exposure of **12** to Martin sulfurane[17] and Luche conditions[18] provided the corresponding allylic alcohol **13**. Treatment of **11** with *p*-toluenesulfonic acid (40 mol%) at 23 °C effected clean elimination to furnish the desired 5-vinyl-1,3-cyclohexadiene **8** (96%). Subsequent heating at 170 °C induced smooth Diels–Alder reaction to afford **7** in excellent yield (98%). Crystallization from *n*-pentane–ethyl acetate enabled single-crystal structure analysis to validate the depicted structure. For the formation of **7** it was crucial to separate the elimination from the cycloaddition step, as cyclopropane ring-opening followed by extrusion of ethylene and aromatization to **14** was observed at elevated temperatures in the presence of acid.[3,19] In this context it is interesting to note that the formed carbocyclic framework was recently also found in natural products isolated from Burmese amber, raising questions about their (biosynthetic) origin.[20] For the cleavage of the cyclic boronic ester, **7** was treated with potassium bifluoride (20.0 equiv) to give diol **15** (47%). Unreacted starting material was recovered (39%) and resubmitted to the reaction conditions to provide **15** in 72% overall yield after three cycles. Having gained access to **15** also enabled investigation of the limitation of oxetane formation based on nucleophilic substitution.[21] Attempts to initiate ring-closure of diol **15** or its C6-keto derivative by protonation, halogenation or epoxidation of the C9–C11 alkene were met with failure. In most cases, unreacted starting material was recovered and decomposition prevailed under more forcing conditions.

For the selective alkene reduction of **15**, Shenvi's direct hydrogen atom transfer (HAT) protocol[22] was identified to be method of choice. Under these conditions ($Mn(dpm)_3$, $PhSiH_3$, *t*-BuOOH, 23 °C) hydrogenolysis of the cyclopropane was not observed and **16** was isolated in 75% yield as a single diastereomer at C9 together with only minor amounts of diastereomerically pure triol **17** (22%, *vide infra*).

Completion of the synthesis of mitrephorone B (**2**) involved oxidation (tetrapropylammonium perruthenate (TPAP), NMO, 4 Å molecular sieves) of **16** to **18** (77%), removal of the tertiary alcohol using samarium(II) iodide (74%)[4,23] and installation of the 1,2-diketone (SeO_2, 100 °C, 1,4-dioxane).[24] The analytical data obtained for synthetic mitrephorone B (**2**) were in full agreement with those reported for the natural material.

Having secured ample amounts of **2**, we set out to test the feasibility of the bio-inspired C–H oxidation to **1**. Gratifyingly, exposure of mitrephorone B (**2**) to the White–Chen catalyst system (25 mol% Fe(*R*,*R*)-PDP, H_2O_2, AcOH, MeCN, 23 °C, 1 h) afforded mitrephorone A (**1**) in 60% yield.[25] To the best of our knowledge, this represents the first example of oxetane formation via C–H oxidation. The use of the enantiomeric Fe(*S*,*S*)-PDP catalyst appears to represent the mismatched case for this C–H oxidation and only 30% of mitrephorone A (**1**) were obtained. In the absence of the iron catalyst, no oxidation was observed. In addition, we were also able to access **1** by electrochemical oxidation of **2** (49%) using the protocol described by Baran (quinuclidine, Me_4NBF_4, RVC foam anode, Ni cathode, 0.2 mA, 1.4–1.7 V, 2 F/mol, HFIP, MeCN, 23 °C, 4 h).[26] Alternatively, applying photocatalysis (TBADT, aq. HCl; 365 nm)[27] we observed significantly lower yields of **1** (14%).

We found that the presence of the enol is crucial to furnish the oxetane. All attempts to effect oxetane formation employing the α-hydroxyketone **18** failed, and only decomposition was observed or starting material was recovered. Further insight was obtained by investigating the iron-mediated C–H oxidation of known diosphenol **20**.[5] For this purpose, triol **17** was first converted to **19** in four steps. Exposure of **19** to tris(dimethylamino)sulfonium difluorotrimethylsilicate (TASF) liberated the tertiary alcohol and induced tautomerization to give **20**. This intermediate was subjected to the White–Chen system as before to promote cyclization to mitrephorone A (**1**) in 13%.[28]

The selectivity towards oxetane formation of **2** might be a result of the short distance between C5 of the enol and H9 (2.64 Å). In agreement with the literature, we believe that the sequence is initiated by oxidation of the enone to a tertiary radical.[26,29] The subsequent incorporation of oxygen might occur directly at C5 or, after radical translocation,[30] at C9. Final ring-closure to the oxetane can occur for both pathways (see Supporting Information for details).

Scheme 2. Total Synthesis of Mitrephorone B (2) and Mitrephorone A (1)[a]

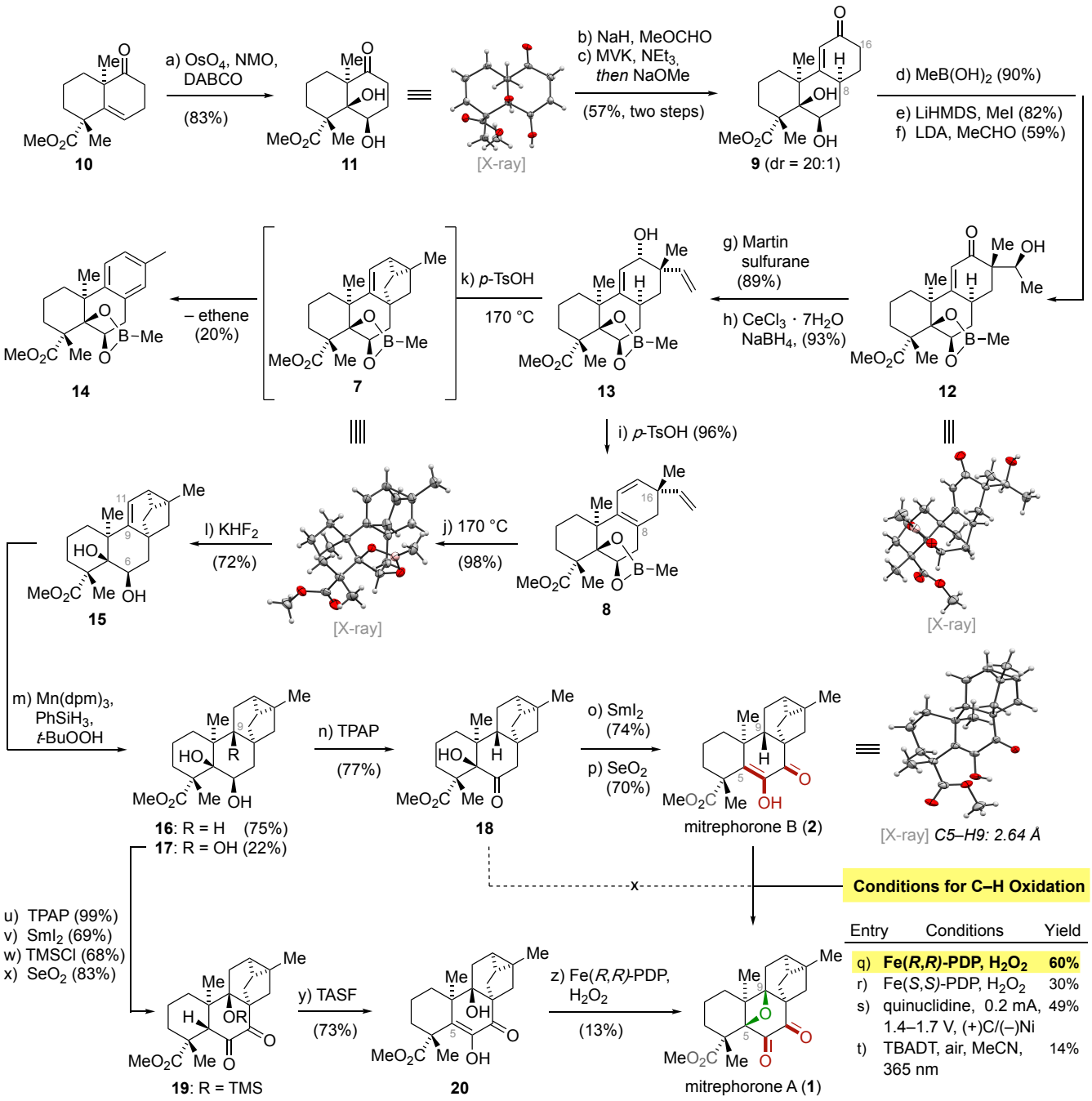

[a]Reagents and conditions: (a) OsO_4, NMO, DABCO, acetone–H_2O, 90 °C, 72 h, 83%; (b) NaH, *then* MeOCHO, THF–PhMe, 0 °C to 23 °C, 4 h; (c) MVK, NEt_3, CH_2Cl_2, 23 °C, 96 h, *then* NaOMe, MeOH, 44 °C, 4 h, 57% over two steps; (d) $MeB(OH)_2$, C_6H_6, 30 °C, 2 h, 90%; (e) LiHMDS, *then* MeI, THF, –50 °C to 23 °C, 13 h, 82%; (f) LDA, TMEDA, *then* MeCHO, THF, –20 °C to –78 °C, 3 h, 59%; (g) Martin sulfurane, C_6H_6, 23 °C, 2 h, 89%; (h) $NaBH_4$, $CeCl_3$•$7H_2O$, MeOH, 0 °C, 3 h, 93%; (i) *p*-TsOH, 4 Å MS, PhMe, 23 °C, 40 h, 96%; (j) PhMe, 170 °C, 3 h, 98%; (k) *p*-TsOH, 4 Å MS, PhMe, 23 °C to 170 °C, 72 h, 20%; (l) KHF_2, MeOH–H_2O, 40 °C, 24 h, 72% over three cycles; (m) $Mn(dpm)_3$, $PhSiH_3$, *t*-BuOOH, *i*-PrOH, 23 °C, 17 h, 97%; (n) TPAP, NMO, 4 Å MS, CH_2Cl_2, 23 °C, 3 h, 77%; (o) SmI_2, THF–MeOH, 23 °C, 20 min, 74%; (p) SeO_2, 1,4-dioxane, 100 °C, 7 h, 70%; (q) Fe(*R*,*R*)-PDP, H_2O_2 (aq.), AcOH, MeCN, 23 °C, 1 h, 60%; (r) Fe(*S*,*S*)-PDP, H_2O_2 (aq.), AcOH, MeCN, 23 °C, 1 h, 30%; (s) (+)RVC foam/(–)Ni, Me_4NBF_4, quinuclidine, air, HFIP, MeCN, 0.2 mA, 23 °C, 4 h, 49%; (t) TBADT, HCl (aq.), 365 nm, 23 °C, 9 h, 14%; (u) TPAP, NMO, CH_2Cl_2, 23 °C, 3 h, 99%; (v) SmI_2, THF–MeOH, 23 °C, 12 min, 69%; (w) TMSCl, DMAP, imidazole, DMF, 90 °C, 6 d, 68%; (x) SeO_2, 1,4-dioxane, 100 °C, 2 h, 83%; (y) TASF, H_2O, DMF, 0 °C; 30 min, 73%; (z) Fe(*R*,*R*)-PDP, H_2O_2 (aq.), AcOH, MeCN, 23 °C, 1 h, 13%.

In summary, we were able to mimic a bio-inspired C–H oxidation of mitrephorone B (**2**) to mitrephorone A (**1**) using either iron-catalysis or electrochemical oxidation. Despite a careful screen of oxidants as well as literature precedence for structurally related substrates,[25,26] oxidation of the C2-position to give mitrephorone C (**3**) was never observed.[31] Our inability to realize this transformation might reveal current limitations of modern C–H oxidation methods or indicate an alternative biosynthetic pathway. For the latter scenario, oxidation of C2 would precede formation of the delicate diosphenol motif thus ruling out mitrephorone B (**2**) as the parent compound.[32]

ASSOCIATED CONTENT

Supporting Information

The Supporting Information is available free of charge on the ACS Publications website.
Experimental details and spectroscopic data (PDF)
X-ray crystallographic data for **2**, **7**, **11**, and **12** (ZIP)

AUTHOR INFORMATION

Corresponding Author

*thomas.magauer@uibk.ac.at

ORCID

Thomas Magauer: 0000-0003-1290-9556

Notes

The authors declare no competing financial interest.

ACKNOWLEDGMENT

This work was supported by the Austrian Science Fund FWF (P31023-NBL to T.M.) and the Center for Molecular Biosciences CMBI. Furthermore, we thank Dr. Kevin Mellem (Maze Therapeutics) and Dr. Cedric Hugelshofer (Merck) for assistance during the preparation of this paper, Juri Skotnitzki (LMU Munich) for chiral GC analysis and Dr. Matthias Schmid (University of Innsbruck) for helpful discussions.

REFERENCES

(1) (a) Hanson, J. R. Diterpenoids. *Nat. Prod. Rep.* **2006**, *23*, 875–885. (b) Hanson, J. R. Diterpenoids. *Nat. Prod. Rep.* **2007**, *24*, 1332–1341. (c) Roy, A.; Roberts, F. G.; Wilderman, P. R.; Zhou, K.; Peters, R. J.; Coates, R. M. 16-Aza-*ent*-beyerane and 16-Aza-*ent*-trachylobane: potent mechanism-based inhibitors of recombinant *ent*-kaurene synthase from Arabidopsis thaliana. *J. Am. Chem. Soc.* **2007**, *129*, 12453–12460.

(2) Li, C.; Lee, D.; Graf, T. N.; Phifer, S. S.; Nakanishi, Y., Burgess, J. P.; Riswan, S.; Setyowati, F. M.; Saribi, A. M.; Soejarto, D. D.; Farnsworth, N. R.; Falkinham III, J. S.; Kroll, D. J.; Kinghorn, A. D.; Wani, M. C.; Oberlies, N. H. A Hexacyclic e*nt*-Trachylobane Diterpenoid Possessing an Oxetane Ring from Mitrephora glabra. *Org. Lett.* **2005**, *7*, 5709–5712.

(3) Hong, Y. J.; Tantillo, D. J. Formation of beyerene, kaurene, trachylobane, and atiserene diterpenes by rearrangements that avoid secondary carbocations. *J. Am. Chem. Soc.* **2010**, *132*, 5375–5386.

(4) (a) Hugelshofer, C. L.; Magauer, T. A Bioinspired Cyclization Sequence Enables the Asymmetric Total Synthesis of Dictyoxetane. *J. Am. Chem. Soc.* **2016**, *138*, 6420–6423. (b) Hugelshofer, C. L.; Magauer, T. A Divergent Approach to the Marine Diterpenoids (+)-Dictyoxetane and (+)-Dolabellane V. *Chem. Eur. J.* **2016**, *22*, 15125 –15136.

(5) Richter, M. J. R.; Schneider, M.; Brandstätter, M.; Krautwald, S.; Carreira, E. M. Total Synthesis of (–)-Mitrephorone A. *J. Am. Chem. Soc.* **2018**, *140*, 16704–16710.

(6) (a) Burkhard, J. A.; Wuitschik, G.; Rogers-Evans, M.; Müller, K.; Carreira, E. M. Oxetanes as versatile elements in drug discovery and synthesis. *Angew. Chem. Int. Ed.* **2010**, *49*, 9052–9067.

(b) Bull, J. A.; Croft, R. A.; Davis, O. A.; Doran, R.; Morgan, K. F. Oxetanes: Recent Advances in Synthesis, Reactivity, and Medicinal Chemistry. *Chem. Rev.* **2016**, *116*, 12150–12233.

(7) Gutekunst, W. R.; Baran, P. S. C–H functionalization logic in total synthesis. *Chem. Soc. Rev.* **2011**, *40*, 1976–1991.

(8) Abrams, D. J.; Provencher, P. A.; Sorensen, E. J. Recent applications of C–H functionalization in complex natural product synthesis. *Chem. Soc. Rev.* **2018**, *47*, 8925–8967.

(9) (a) Ng, S. M.; Beaudry, C. M.; Trauner, D. Intramolecular Diels-Alder reactions of 5-vinyl-1,3-cyclohexadienes. *Org. Lett.* **2003**, *5*, 1701–1704. (b) Kelli, S. K.; Beaudry, C. M.; Trauner, D.; Houk, K.N. Dienophile Twisting and Substituent Effects Influence Reaction Rates of Intramolecular Diels−Alder Cycloadditions: A DFT Study. *J. Am. Chem Soc.* **2005**, *127*, 3688–3689.

(10) Gallier, F.; Martel, A.; Dujardin, G. Enantioselective Access to Robinson Annulation Products and Michael Adducts as Precursors. *Angew. Chem. Int. Ed.* **2017**, *56*, 12424–12458.

(11) Deschamp, J.; Hermant, T.; Riant, O. An easy route toward enantioenriched polycyclic derivatives via an asymmetric domino conjugate reduction–aldol cyclization catalyzed by a chiral Cu(I) complex. *Tetrahedron* **2012**, *68*, 3457–3467.

(12) Zhou, B.; Miao, Z.; Deng, G.; Ding, J.; Yang, Y.; Feng, H.; Li, Y. Synthesis and biological evaluation of novel triptolide analogues for anticancer activity. *Bioorg. Med. Chem. Lett.* **2010**, *20*, 6217–6221.

(13) (a) Yu, J.; Yu, B. Synthesis of the ABC skeleton of the aglycon of Echinoside A. *Chin. Chem. Lett.* **2015**, *26*, 1331–1335. (b) Utilizing alkene **10** under identical reaction conditions did not provide the Robinson product, but lead to a complex product mixture.

(14) Xu, C.; Han, A.; Virgil, S. C.; Reisman, S. E. Chemical Synthesis of (+)-Ryanodine and (+)-20-Deoxyspiganthine. *ACS Cent. Sci.* **2017**, *3*, 278–282.

(15) Chieffi, A.; Kamikawa, K.; Ahman, J.; Fox, J. M.; Buchwald, S. L. Catalytic asymmetric vinylation of ketone enolates. *Org. Lett.* **2001**, *3*, 1897–1900.

(16) Corey, E. J.; Cheng, X.-M. *Logic of chemical synthesis*; Wiley: New York, **1995**.

(17) Kuramochi, A.; Usuda, H.; Yamatsugu, K.; Kanai, M.; Shibasaki, M. Total synthesis of (±)-garsubellin. *J. Am. Chem. Soc.* **2005**, *127*, 14200–14201.

(18) Ramesh, R.; Bell, V.; Twidle, A. M.; Gonnade, R.; Reddy, D. S. Enantiospecific Synthesis of Both Enantiomers of the Longtailed Mealybug Pheromone and Their Evaluation in a New Zealand Vineyard. *J. Org. Chem.* **2015**, *80*, 7785–7789.

(19) Wu, Z.-Y.; Zhang, Y.-B.; Zhu, K.-K.; Luo, C.; Zhang, J.-X.; Cheng, C.-R.; Feng, R.-H.; Yang, W.-Z.; Zeng, F.; Wang, Y.; Xu, P.; Guo, J.; Liu, X.; Guan, S.; Guo, D. Anti-inflammatory diterpenoids from the root bark of Acanthopanax gracilistylus. *J. Nat. Prod.* **2014**, *77*, 2342–2351.

(20) Shimizu, E.; Koshino, H.; Noro, A.; Maruyama, M.; Shimoda, N.; Uesugi, S.; Ohnishi, M.; Kimura, K. Isolation of a spirolactone norditerpenoid as a yeast Ca^{2+} signaltransduction inhibitor from Kuji amber and evaluation of its effects on PPM1A activity. *Filoterapia* **2019**, *134*, 290–296.

(21) (a) Sigrist, R.; Rey, M.; Dreiding, A. S. Kurze Totalsynthesen von (±)-Sativen und *(±)-cis*-Sativendiol. *Helv. Chim. Acta* **1988**, *71*, 788–807.

(b) Galatsis, P.; Parks, D. J. Stereoselective synthesis of substituted oxetanes. *Tet. Lett.* **1994**, *35*, 6611–6614.

(22) Iwasaki, K.; Wan, K. K.; Oppedisano, A.; Crossley, S. W. M.; Shenvi, R. A. Simple, chemoselective hydrogenation with thermodynamic stereocontrol. *J. Am. Chem. Soc.* **2014**, *136*, 1300–1303.

(23) Efforts to deoxygenate **16** via a pinacol-like rearrangement remained unsuccessful. For recent examples, see: (a) Defaut, B.; Parsons, T. B.; Spencer, N.; Male, L.; Kariuki, B. M.; Grainger, R. S. Synthesis of the transhydrindane core of dictyoxetane. *Org. Biomol. Chem.* **2012**, *10*, 4926–4932. (b) Liu, S.-A.; Trauner, D. Asymmetric Synthesis of the Antiviral Diterpene Wickerol A. *J. Am. Chem. Soc.* **2017**, *139*, 9491–9494.

(24) Riley, H. L. Oxidation Activity of Selenium Dioxide. *Nature* **1947**, *159*, 571–572.

(25) Chen, M. S.; White, M. C. Combined effects on selectivity in Fe-catalyzed methylene oxidation. *Science* **2010**, *327*, 566–571.

(26) Kawamata, Y.; Yan, M.; Liu, Z.; Bao, D.-H.; Chen, J.; Starr, J. T.; Baran, P. S. Scalable, Electrochemical Oxidation of Unactivated C–H Bonds. *J. Am. Chem. Soc.* **2017**, *139*, 7448–7451.

(27) Laudadio, G.; Govaerts, S.; Wang, Y.; Ravelli, D.; Koolman, H. F.; Fagnoni, M.; Djuric, S. W.; Noël, T. Selective C(sp^3)-H Aerobic Oxidation Enabled by Decatungstate Photocatalysis in Flow. *Angew. Chem. Int. Ed.* **2018**, *57*, 4078–4082.

(28) Electrochemical oxidation of diosphenol **20** provided **1** in 28% yield.

(29) (a) Dantignana, V.; Serrano-Plana, J.; Draksharapu, A.; Magallón, C.; Banerjee, S.; Fan, R.; Gamba, I.; Guo, Y.; Que, L. Jr.; Costas, M. Company, A. Spectroscopic and Reactivity Comparisons between Nonheme Oxoiron(IV) and Oxoiron(V) Species Bearing the Same Ancillary Ligand. *J. Am. Chem. Soc.* **2019**, *141*, 15078–15091. (b) White, M. C.; Zhao, J. Aliphatic C−H Oxidations for Late-Stage Functionalization. *J. Am. Chem. Soc.* **2018**, *140*, 13988–14009.

(30) (a) Robertson, J.; Pillai, J.; Lush, R. K. Radical translocation reactions in synthesis. *Chem. Soc. Rev.* **2001**, *30*, 94–103. (b) Hioe, J.; Zipse, H. Radical stability and its role in synthesis and catalysis. *Org. Biomol. Chem*., **2010**, *8*, 3609–3617.

(31) We also attempted C–H oxidation of alkene **7**, but only observed formation of a complex product mixture.

(32) The recent isolation of a series of closely related natural products corroborates this hypothesis: Dal Piaz, F.; Bader, A.; Malafronte, N.; D'Ambola, M.; Petrone, A. M.; Porta, A.; Ben Hadda, T.; Tommasi, N. de; Bisio, A.; Severino, L. Phytochemistry of compounds isolated from the leaf-surface extract of Psiadia punctulata (DC.) Vatke growing in Saudi Arabia. *Phytochemistry* **2018**, *155*, 191–202.

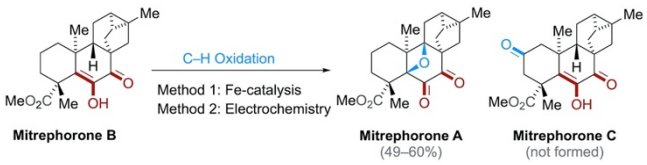

Mitrephorone B

Mitrephorone A
(49–60%)

Mitrephorone C
(not formed)